

1996

# The Simplest Subdivision Scheme for Smoothing Polyhedra

Jörg Peters

Ulrich Reif

Report Number:  
96-032

---

Peters, Jörg and Reif, Ulrich, "The Simplest Subdivision Scheme for Smoothing Polyhedra" (1996). *Computer Science Technical Reports*. Paper 1287.

<http://docs.lib.purdue.edu/cstech/1287>

This document has been made available through Purdue e-Pubs, a service of the Purdue University Libraries. Please contact [epubs@purdue.edu](mailto:epubs@purdue.edu) for additional information.

**THE SIMPLEST SUBDIVISION  
SCHEME FOR SMOOTHING POLYHEDRA**

**Jorg Peters  
Ulrich Reif**

**Department of Computer Science  
Purdue University  
West Lafayette, IN 47907**

**CSD-TR 96-032  
May 1996**

# The simplest subdivision scheme for smoothing polyhedra

Jörg Peters \*      Ulrich Reif†

August 19, 1996

## Abstract

Given a polyhedron, construct a new polyhedron by connecting every edge-midpoint to its four neighboring edge-midpoints. This refinement rule yields a  $C^1$  surface and the surface has a piecewise quadratic parametrization except at finite number of isolated points. We analyze and improve the construction.

Mathematics of Surfaces ed J A Gregory pp279-280 Clarendon Press, Oxford 1986  
ISBN 0 19 853609 7 -

## 1 Introduction

Consider an input polyhedron with not necessarily planar facets. The simplest subdivision scheme connects every edge-midpoint to the four midpoints of the edges that share both a vertex and a face with the current edge. Once all midpoints are linked, the old mesh is discarded. Figure 1 shows the process. Each subdivision step can be interpreted as cutting off all vertices including with each a neighborhood that reaches out to the midpoints of the emanating edges. The cuts are in general not planar.

Since the subdivision mask consists of only two points and there is only one rule regardless of the connectivity of the polyhedron, the subdivision scheme is as simple as it can be. It is called *midedge subdivision* hereafter. We will show in Section 2 that it is a factored box-spline subdivision and hence a close relative of the modified box-spline subdivisions [3], [2], [4] of Doo and Sabin, Catmull and Clark, and Loop. Section 3 and the Appendix establish the smoothness of the limit surface and Section 4 specifies a modified midedge subdivision with improved convergence rate. The complete analysis of the smoothness of the limit surface is remarkable, because only recently, after 30

---

\*Supported by NSF NYI grant 9457806-CCR

†Supported by BMBF Projekt 03-HO7STU-2.

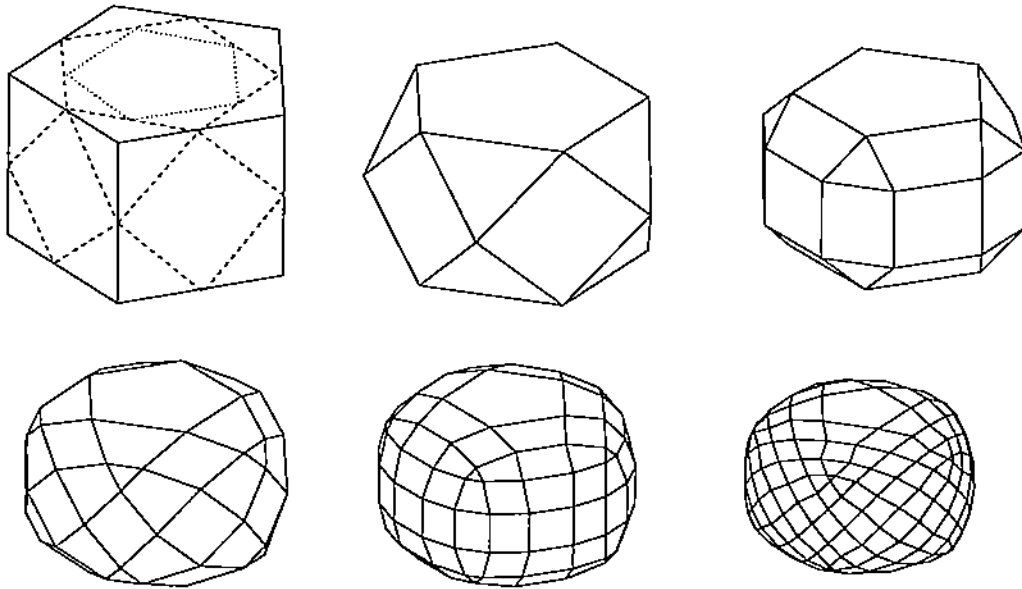


Figure 1: Midpoint subdivision at work.

years, the smoothness (and for some parameter choices the lack of smoothness) of the subdivision surfaces defined by [3] and [2] has been rigorously established in [6].

## 2 Quadratic parametrization

At each step, a subdivision algorithm creates a new mesh of points from an old mesh. A desirable property of any subdivision algorithm is that it generates increasing regions whose points all have the same valence and whose facets all have the same number of edges. A submesh of points and facets with this standard valence and number of edges is called *regular*. Specific subdivision rules like those of Doo and Sabin or Catmull and Clark or Loop derive their appeal from the fact that the limit surface is explicitly known for regular meshes; the limit surfaces are respectively biquadratic tensor-product spline surfaces, bicubic tensor-product spline surfaces and surfaces formed as a linear combination of shifts of a 3-direction box spline. In midedge subdivision every new non-boundary point has exactly four neighbors, and every mesh point is replaced by a quadrilateral. A regular submesh consists therefore of quadrilaterals and 4-valent points. On this mesh a surface formed as a linear combination of the shifts of the 4-direction box spline, called the Zwart-Powell element ([9],[7]), is defined by the following subdivision process (c.f. [1]).

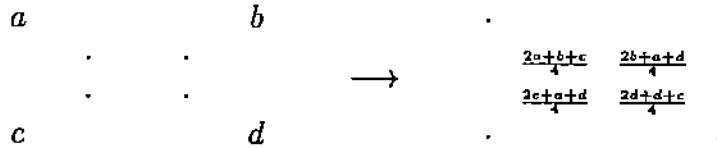


Figure 2: Four-direction box spline subdivision.

At each step replicate each coefficient with index  $i, j$  in a new array at positions  $2i, 2j, 2i + 1, 2j, 2i, 2j + 1$ , and  $2i + 1, 2j + 1$ . Then average in the new array first all entries  $i, j$  with  $i + 1, j + 1$  and then all entries  $i, j$  with  $i - 1, j + 1$ . Figure 2 shows the result of the averaging process: for each quadrilateral each of four new points is obtained by taking  $1/2$  of one point and  $1/4$  of each of its two neighbors.

**Theorem 1** *On a regular mesh, midedge subdivision converges to a surface parametrized by shifts of the 4-direction box-spline.*

**Proof** Two steps of the midedge subdivision equal one step of the 4-direction box-spline subdivision.  $\square$

Since we know the limit surface for regular mesh regions, we will in the following always combine two steps of midedge subdivision and refer to it as a double-step. The double-step rule is efficiently represented by the mask

$${}^{1/4} \begin{array}{c} 1 \\ 2 \quad 1 \end{array}$$

which applies to a vertex and its two neighbors in the same facet. Note that in contrast to the Doo-Sabin and other subdivision masks, the (double) midedge subdivision mask is not parametrized by the valence  $n$  of the particular point, but is uniform for all configurations.

For later use, we note that any submesh of 9 coefficients  $B_\ell, B'_\ell, B''$ ,  $\ell = 0..3$  of the 4-direction box spline control-point mesh defines four polynomials in Bernstein-Bézier form with coefficients  $b_{ijk}^\ell$ ,  $i + j + k = 2$ ,  $\ell = 0..3$ . The generic layout of the coefficients and the algebraic correspondence are shown in Figure 3. In particular, if  $B_\ell = B'_\ell = 0$ , for  $\ell = 0..3$  and  $B'' = 1$ , we obtain the definition of a single 4-direction box-spline in terms of the Bernstein-Bézier form (see Figure 4).

### 3 Smoothness at extraordinary points

Since each midedge subdivision double-step replaces points and edges by quadrilaterals, the new mesh at each step is regular except for a fixed number of increasingly separated

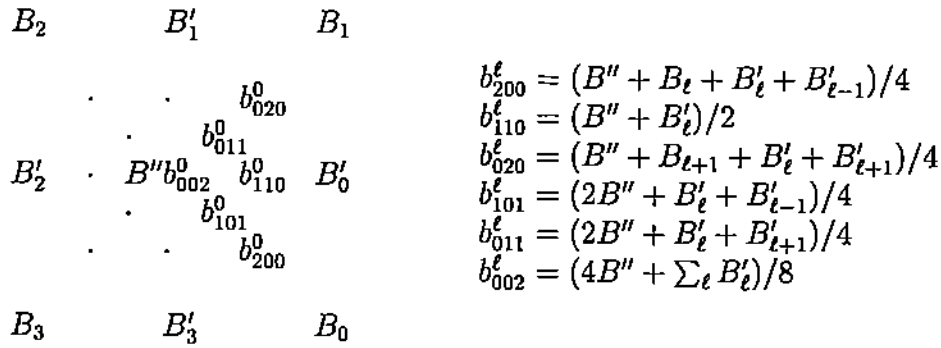


Figure 3: Correspondence of box spline coefficients and Bernstein-Bézier coefficients.

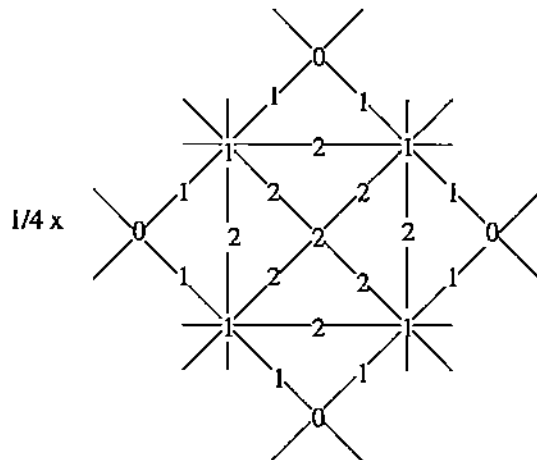


Figure 4: Bernstein-Bézier representation of the four-direction box spline.

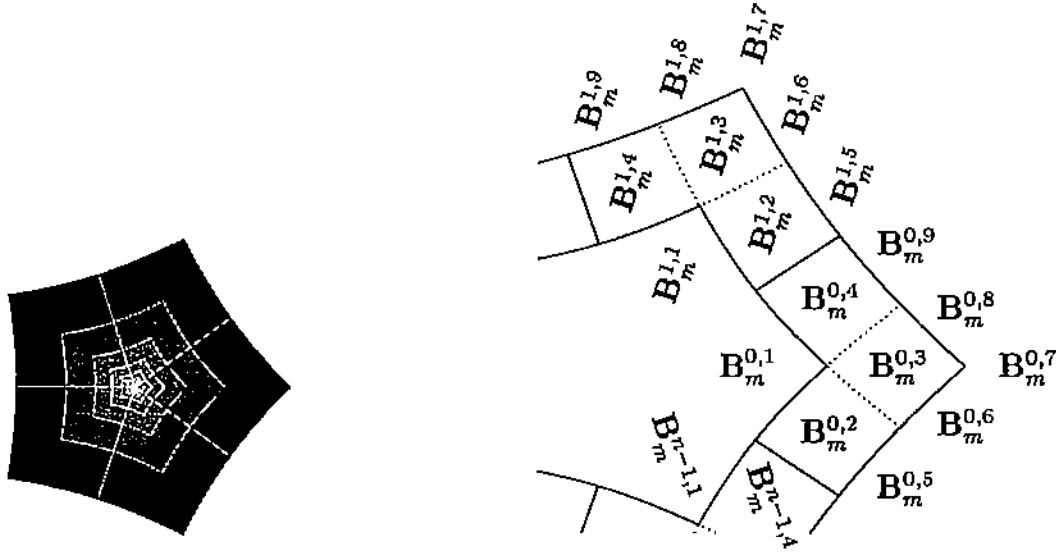


Figure 5: Union of surface layers at an extraordinary point and labeling of control points.

non-four-sided mesh facets. We consider one such facet (cf. Figure 5). At each step the polygon defining the facet contracts, converging towards the average of the points. To confirm the smoothness at this extraordinary point, we analyze the local *subdivision matrix* that maps  $k$  layers of old points surrounding the extraordinary point to  $k$  layers of new points. For almost all inputs, the eigenvalues and eigenvectors of the subdivision matrix determine the smoothness of the limit surface [8].

The conversion to the Bernstein form in the preceding section shows that 3 layers of control points suffice to define a complete new surface layer  $\mathbf{x}_m$  that attaches to a previous layer  $\mathbf{x}_{m-1}$ . The union of all surface layers  $\bigcup_{m \in \mathbb{N}} \mathbf{x}_m$  forms the midedge subdivision surface  $\mathbf{y}$ . Each of the  $n$  segments ( $j \in \mathbb{Z}_n = \{0, \dots, n-1\}$ )

$$\mathbf{x}_m^j : [0, 2]^2 \setminus [0, 1]^2 \rightarrow \mathbb{R}^3$$

that make up the  $m$ th surface layer consists of 12 quadratic Bernstein-Bézier patches, four corresponding to each nine-tuple of control points

$$\mathbf{B}_m^{j,k}, k = 1 : 9, \quad (3.1)$$

$$\mathbf{B}_m^{j,k}, k = 1 : 5, 9, \mathbf{B}_m^{j+1,k}, k = 1, 2, 5, \quad (3.2)$$

$$\mathbf{B}_m^{j,k}, k = 2, 3, 5 : 8, \mathbf{B}_m^{j-1,k}, k = 1, 4, 9. \quad (3.3)$$

The labeling used here is shown in Figure 5. The vector of control points  $\mathbf{B}_m$  that define the  $m$ th surface layer consists of  $n$  blocks of 9 elements, each. The subdivision matrix  $A$  transforms

$$\mathbf{B}_{m+1} = A\mathbf{B}_m = A^{m+1}\mathbf{B}_0.$$

**Lemma 3.1** *The eigenvalues of the subdivision matrix  $A$  are real-valued and form a decreasing sequence starting with*

$$1, \lambda, \lambda, \text{ where } \lambda := \frac{1 + \cos(\frac{2\pi}{n})}{2}.$$

**Proof** Since the scheme is symmetric, i.e. invariant under a rotation of segment labels, we can determine the eigenvalues and eigenvectors conveniently with the help of discrete Fourier transform. Let  $I$  be the identity matrix, and  $W$  the diagonal matrix consisting of  $9 \times 9$  matrices  $W_k$  defined by

$$W = \text{diag}(W_k), \quad W_k := \omega_n^k I_{9 \times 9}, \quad \omega_n := \exp(\sqrt{-1} \frac{2\pi}{n}).$$

The transformed matrix

$$\hat{A} = W^{-1} A W,$$

has the same eigenvalues as  $A$  and a block-diagonal structure  $\hat{A} = \text{diag}(A_k)$  with  $9 \times 9$  submatrices  $\hat{A}^k, k = 0, \dots, n-1$  that are nonzero only in the first four columns:

$$\hat{A}_k(1 : 4, :) = \begin{pmatrix} \hat{\alpha}_k & 0 & 0 & 0 \\ p + \bar{\omega}_n q & q & 0 & 0 \\ p & q & 0 & q \\ p + \omega_n q & 0 & 0 & q \\ q & p & 0 & \bar{\omega}_n q \\ q & p & q & 0 \\ 0 & q & p & q \\ q & 0 & q & p \\ q & \omega_n q & 0 & p \end{pmatrix} \quad (3.4)$$

where  $p := 1/2, q := 1/4$ , and

$$\hat{\alpha}_k = \sum_{i=0}^{n-1} \omega_n^{ik} \alpha_i = \frac{1 + \cos(k \frac{2\pi}{n})}{2}.$$

Evidently the 9 eigenvalues of each submatrix  $\hat{A}_k$  are

$$\hat{\alpha}_k, \frac{1}{4}, \frac{1}{4}, 0, 0, 0, 0, 0, 0$$

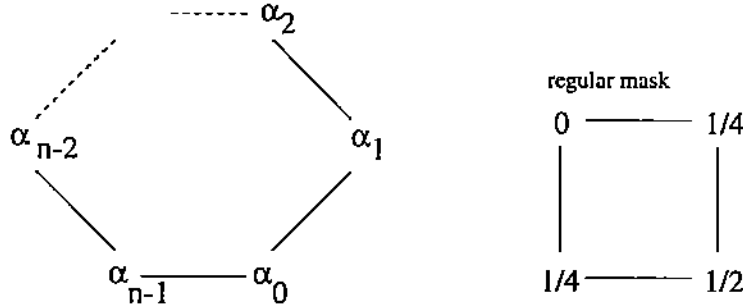
and the combined list of eigenvalues of all submatrices starts with the eigenvalues  $\hat{\alpha}_0 = 1, \hat{\alpha}_1 = \hat{\alpha}_{n-1} = \lambda$ .  $\square$



The single maximal eigenvalue 1 assures convergence to an affinely invariant surface. To verify its smoothness, it suffices to show that the eigenvectors corresponding to the two subdominant eigenvalues define a regular and injective map, namely the characteristic map that parametrizes the tangent plane in the limit point. The details of this proof are in the Appendix.

## 4 Convergence improvement at irregular points

The need for an improvement in the convergence of the midedge subdivision is illustrated by Figure 6. The input data form a cylinder by extruding a 16-gon that is regular except that one of the vertices has been moved above the plane to form a peak. Convergence of the central 16-edge facet is slow. The subdominant eigenvalue  $\lambda = (1 + \cos(\frac{2\pi}{16}))/2 \approx .962$  implies that the distance of a vertex to the centroid of the facet shrinks by less than 4%. Conversely the convergence at the peak is so fast that it seems pointed. This fast convergence of triangular facets is already apparent in Figure 1 where the central triangle shrinks almost to a point in just 3 double-steps.



To even out the speed of convergence, we modify the subdivision mask for  $n$ -sided facets to have weights

$$\alpha_j = 2 \sum_{i=0}^{\bar{n}} 2^{-i} \cos(ji \frac{2\pi}{n}) \text{ where } \bar{n} := \left\lfloor \frac{n-1}{2} \right\rfloor$$

resulting in eigenvalues

$$\hat{\alpha}_i = \hat{\alpha}_{n-i} = 2^{-i}, \quad i = 0.. \bar{n}$$

with  $\hat{\alpha}_{n/2} = 0$  for  $n$  even, consistent with the regular case. Regularity and injectivity of the characteristic map are evident from the coefficients displayed in Figures 11 and 12.

We conclude with three examples of modified midedge subdivision. To distribute the change of normal and keep some features sharp, we parametrize the mask in the first subdivision double-step only as follows (cf. [5]):

$$\begin{array}{ccc} \frac{1-\gamma}{2} & & \\ \gamma & \frac{1-\gamma}{2} & \gamma \in [0.5, 1]. \end{array}$$

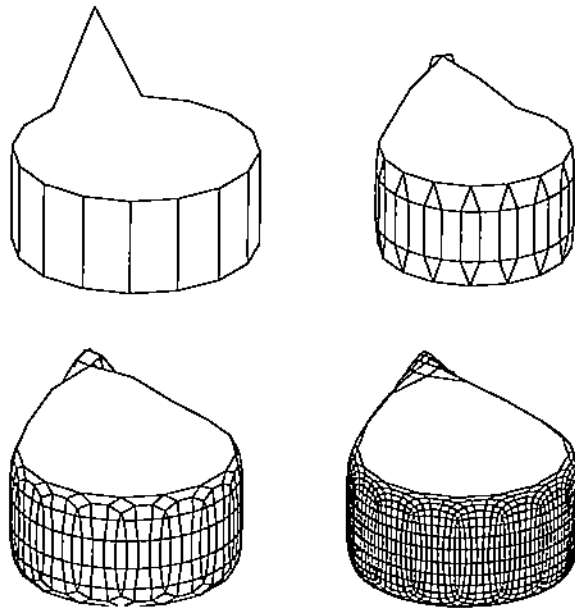


Figure 6: Fast convergence of the midedge subdivision for 3-sided facets and slow convergence for large facets.

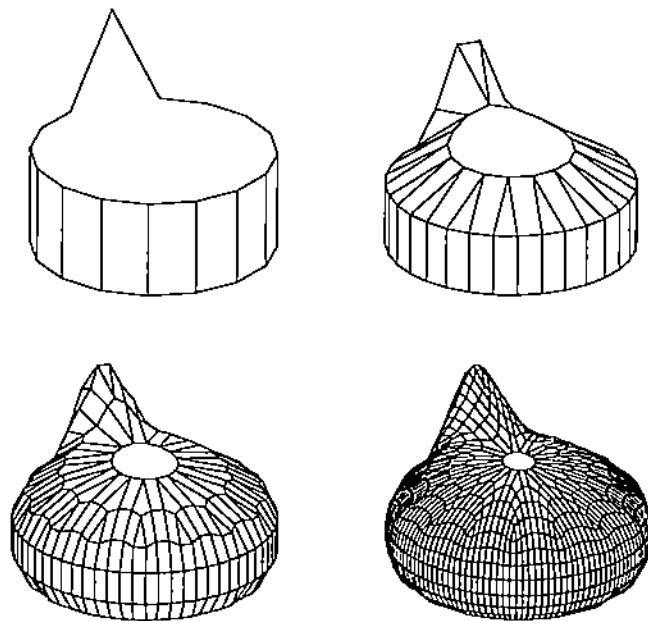


Figure 7: Balanced convergence of the modified midedge subdivision.

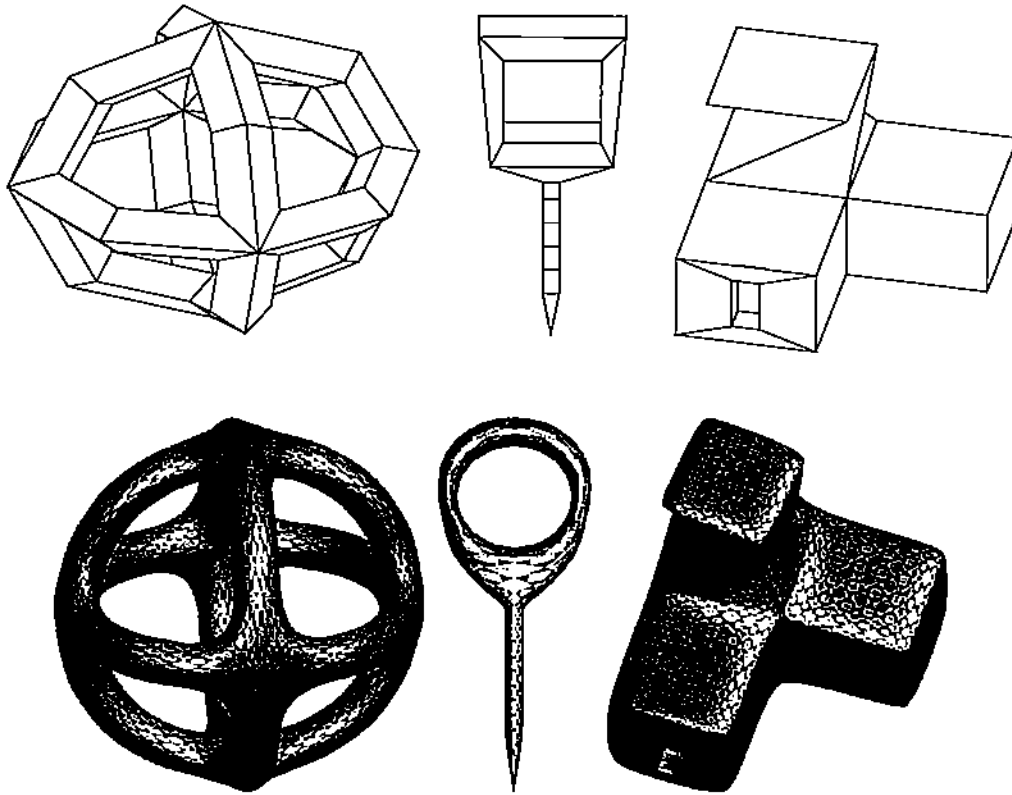


Figure 8: Modified midedge subdivision

In the extreme case, setting  $\gamma = 1$  at a vertex results in a sharp point and setting  $\gamma = 1$  for the two vertices of an edge results in a sharp edge. Conversely, setting  $\gamma = 0.5$  at a point, smoothes maximally. The checker pattern highlights individual triangles on the surfaces.

## References

- [1] BOOR, C. D., HÖLLIG, K., AND RIEMENSCHNEIDER, S. *Box splines*. Springer Verlag, 1994.
- [2] CATMULL, E., AND CLARK, J. Recursively generated B-spline surfaces on arbitrary topological meshes. *Computer Aided Design* 10 (1978), 350–355.
- [3] DOO, D., AND SABIN, M. A. Behaviour of recursive subdivision surfaces near extraordinary points. *Computer Aided Design* 10 (1978), 356–360.

- [4] LOOP, C. Smooth subdivision for surfaces based on triangles. Master's thesis, University of Utah, 1987.
- [5] PETERS, J. Smooth free-form surfaces over irregular meshes generalizing quadratic splines. *Computer Aided Geometric Design* 10 (1993), 347–361.
- [6] PETERS, J., AND REIF, U. Analysis of generalized B-spline subdivision algorithms. Tech. rep., University of Stuttgart, Fachbereich Mathematik, 1996.
- [7] POWELL, M. Piecewise quadratic surface fitting for contour plotting. In *Software for Numerical Mathematics*, D. Evans, Ed. Academic Press, 1969.
- [8] REIF, U. A unified approach to subdivision algorithms near extraordinary vertices. *Computer Aided Geometric Design* 12 (1995), 153–174.
- [9] ZWART, P. Multivariate splines with non-degenerate partitions. *SIAM J. of Numer. Analysis* 10 (1973), 665–673.

## 5 Appendix: Regularity and injectivity of the characteristic map

This section completes the proof started in Section 3, of smoothness of the limit surface at extraordinary points.

Two eigenvalues of the subdivision matrix are *subdominant* if they are either strictly larger in modulus than any eigenvalue other than the unique largest  $\hat{\alpha}_0 = 1$  or, if equal to the fourth largest eigenvalue, their eigenspaces have a strictly higher dimension than those of any other eigenvalue of the same absolute value. In the case of midedge subdivision the subdominant eigenvalues belong to  $\hat{A}_1$  and  $\hat{A}_{n-1}$  and have the value  $\lambda$  since  $\alpha_i > \alpha_j$  for  $i < j < n/2$  and, for  $n > 3$ ,  $\lambda \geq 1/2 > 1/4$ . If  $n = 3$ , then  $\lambda = 1/4$  is an 8-fold eigenvalue but the Jordan decomposition of the matrix shows eigenspaces of multiplicity three for each of  $\hat{A}_1$  and  $\hat{A}_{n-1}$ .

It remains to show regularity and injectivity of the characteristic map. This task is generically proportional to the size of the subdivision mask. Fortunately this is minimal for midedge subdivision. Only recently, in conjunction with the analysis of midedge subdivision, techniques have been developed to prove sharp results for generalized bi-quadratic and bicubic subdivision schemes [6].

**Lemma 5.1** *The characteristic map of midedge subdivision is regular and injective.*

**Proof** The eigenvector corresponding to the subdominant eigenvalues  $\lambda$  is

$$v_\lambda := \begin{pmatrix} \omega_n^0 v \\ \omega_n^1 v \\ \vdots \\ \omega_n^{n-1} v \end{pmatrix} \text{ where } v := \begin{pmatrix} 2 \\ 4 + 2c \\ 6 + 2c \\ 4 + 2c \\ 6 + 4c \\ 8 + 3c \\ 10 + 4c \\ 8 + 3c \\ 6 + 4c \end{pmatrix} + is \begin{pmatrix} 0 \\ -2 \\ 0 \\ 2 \\ -4 \\ -2 \\ 0 \\ 2 \\ 4 \end{pmatrix}, \quad \begin{aligned} c &:= \cos\left(\frac{2\pi}{n}\right) \\ s &:= \sin\left(\frac{2\pi}{n}\right) \end{aligned}$$

By arranging the entries of the eigenvector according to the labeling in Figure 5 and interpreting the real part as  $x$  and the imaginary part as the  $y$  component, we obtain the box spline control points  $\mathbf{B}^{0,k}$  with coordinates

$$x + iy = \begin{pmatrix} 6 + 4c & 8 + 3c & 10 + 4c \\ 4 + 2c & 6 + 2c & 8 + 3c \\ 2 & 4 + 2c & 6 + 4c \end{pmatrix} + is \begin{pmatrix} 4 & 2 & 0 \\ 2 & 0 & -2 \\ 0 & -2 & -4 \end{pmatrix}.$$

The control points are symmetric with respect to the diagonal since midedge subdivision is invariant under reflection. The remaining control points are obtained by multiplication with  $\omega_n^i$ , i.e. rotation by  $2\pi/n$ . To analyze further the map we transform from box spline to Bernstein form. Figure 9 shows one half of one segment of the characteristic map, namely the Bernstein coefficients of six  $C^1$ -connected quadratic pieces. The Jacobian consists, therefore, of six  $C^0$ -connected quadratics. Figure 10 displays the evidently positive coefficients of the Jacobian proving that the characteristic map is regular.

To show injectivity it suffices to show that the boundary of the half-segment is injective (c.f. [6]). The boundary of a half-segment consists of the images  $l_1$ ,  $l_2$ ,  $l_3$  and  $l_4$  of the segments  $(1, 0)$ ,  $(2, 0)$ ,  $(2, 0)$ ,  $(2, 2)$ ,  $(2, 2)$ ,  $(1, 1)$ , and  $(1, 1)$ ,  $(1, 0)$  under the characteristic map. Both  $l_1$  and  $l_3$  are regular line segments, along the  $x$ -axis and the ray with slope  $(1 + c, -s)$  respectively, while  $l_2$  is a  $\lambda^{-1}$ -scaled, subdivided copy of the regular parabolic segment  $l_4$ . Regular parabolas do not self-intersect. Hence we need only check for pairwise intersections of the boundary curves. Since all other segments are confined to the negative  $y$ -halfplane  $l_3$  does not intersect them. Since the middle coefficient of  $l_4$  lies on the ray  $(3(1 + c), -s)$  through the origin between the rays of  $l_1$  and  $l_3$  neither  $l_2$  nor  $l_4$  can intersect either  $l_1$  or  $l_3$ . Lastly,  $l_2$  and  $l_4$  do not intersect, because  $\lambda \neq 1$ .  $\square$

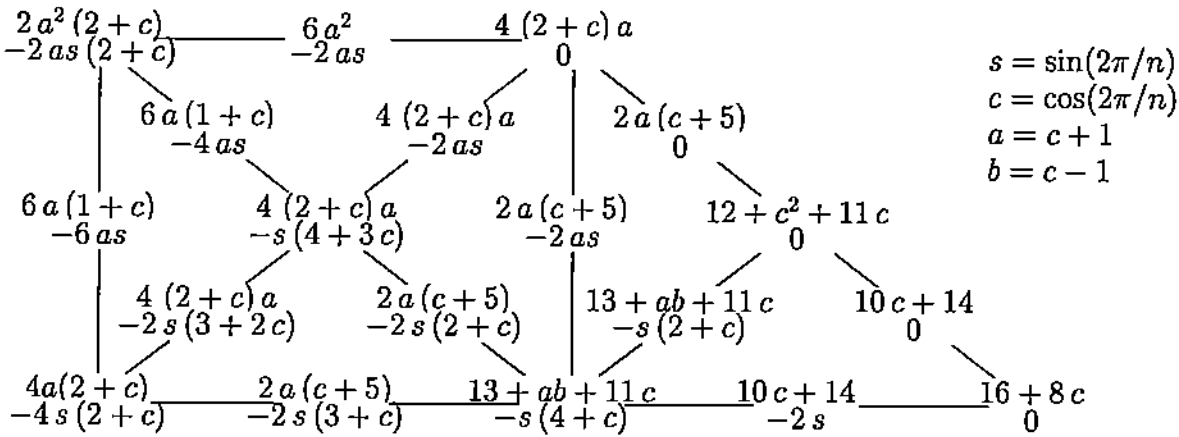
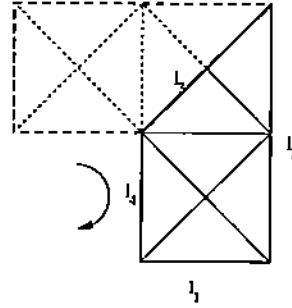


Figure 9: Characteristic map of midedge subdivision.

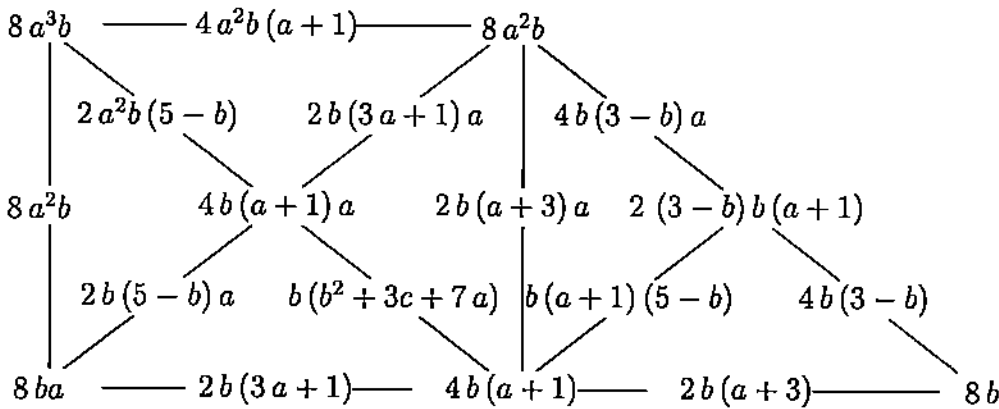


Figure 10: Scaled Jacobian of the characteristic map of midedge subdivision.

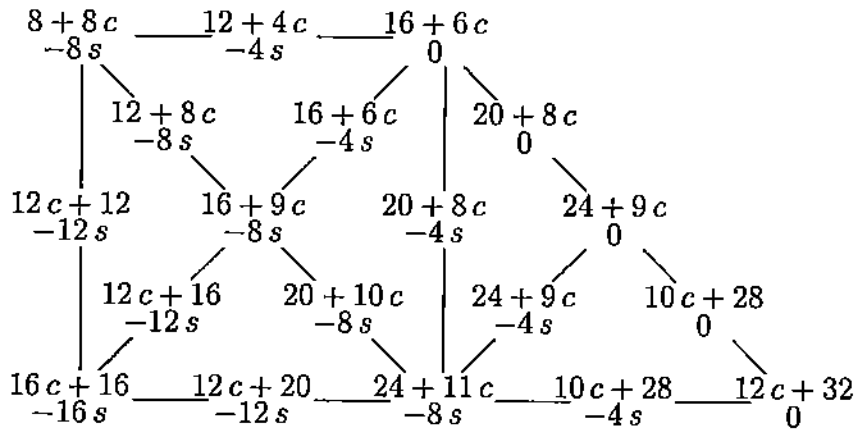


Figure 11: Characteristic map of modified midedge subdivision.

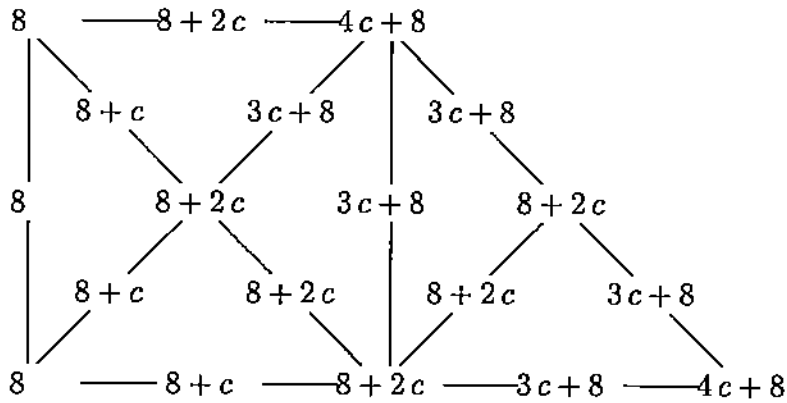


Figure 12: Scaled Jacobian of the characteristic map of modified midedge subdivision.